Double-difference earthquake relocation using waveform cross-correlation in Central and East Java, Indonesia s

Faiz Muttaqy,[1] Andri Dian Nugraha,[2] Nanang T. Puspito,[2] David P. Sahara,[2] Zulfakriza Zulfakriza,[2] Supriyanto Rohadi,[3] Pepen Supendi[3]

[1]Graduate Program of Geophysical Engineering, Faculty of Mining and Petroleum Engineering, Institut Teknologi Bandung, Jalan Ganesha No. 10, Bandung 40132, Indonesia
e-mail: *faiz.muttaqy@yahoo.com*

[2]Global Geophysics Research Group, Faculty of Mining and Petroleum Engineering, Institut Teknologi Bandung, Jalan Ganesha No. 10, Bandung 40132, Indonesia

[3]Agency for Meteorology, Climatology and Geophysics (BMKG), Jakarta, Indonesia

Abstract The Central and East Java region, which is part of the Sunda Arc, has relatively high seismic rates due to the convergence of two major tectonic plates in the Indonesian region; i.e., the Indo-Australian Plate subducting under the Eurasian Plate. Many devastating earthquakes have occurred in this area as a result of the interaction between these two plates. Two examples are the 1994 Banyuwangi earthquake (Mw 7.6) and the 2006 Yogyakarta earthquake (Mw 6.3). This study aims to determine precise earthquake locations and analyze the pattern of seismic distribution in Central and East Java, Indonesia. We manually re-picked P and S-wave arrival times that were recorded by the Agency for Meteorology, Climatology and Geophysics (BMKG) of the Indonesian earthquake network during the time period January 2009 to

September 2017. We then determined the earthquake locations using a non-linear method. To improve the accuracy of the earthquake locations, we relocated 1,127 out of 1,529 events, using a double-difference algorithm with waveform cross-correlation data. Overall, the seismicity in the Central and East Java region is predominantly distributed in the south of Java Island; e.g., the Kebumen, Yogyakarta, Pacitan, Malang, and Banyuwangi clusters. These clusters are probably related to the subduction activity in these regions. Meanwhile, there are clusters of earthquakes having shallow depths on the mainland that indicate the activity of inland faults in the region; e.g., the Opak Fault, the Kendeng Thrust, and the Rembang-Madura-Kangean-Sakala (RMKS) Fault Zone. Several other active inland faults have not shown any significant seismicity over the time period mentioned, i.e., the Pasuruan Fault, the Lasem Fault, the Muria Fault, the Semarang Thrust, and the Probolinggo Fault.

Keywords: Hypocenter determination, 1-D seismic velocity model, waveform cross-correlation, relocation, Central Java, East Java

1 Introduction

Central and East Java are part of the Sunda Arc, which has relatively high seismicity and a complex geological system as a result of the Indo-Australian Plate subducting under the Eurasian Plate. The convergence rate varies from ~5.6 cm/yr in the western part of Java to ~6.5 cm/yr in the eastern part (Koulali et al. 2017). This has produced several active faults, i.e., the Semarang Thrust Fault, the Kendeng Thrust Fault, the Opak Fault, the Lasem Fault, the Probolinggo Fault and the Pasuruan Fault, as well as the volcanoes that most likely control the

seismicity in the study area (Marliyani, 2016; Pusat Studi Gempa Nasional (PuSGeN), 2017) (Fig.1). In contrast with the oblique convergence that occurs in Sumatra, the convergence is normal in the western part of the Sunda Arc up to the plate boundaries at Java Island (Malod et al., 1995). Consequently, the seismic rate in Central and East Java is relatively lower than in Sumatra and West Java (the transitional zone from oblique to normal subduction) (Newcomb and Mccann, 1987). However, the study area still has a potential for destructive earthquakes since the seismic gap that is found in this area threatens the region with potential future megathrust events (Widiyantoro et al., 2020). Based on historical earthquake data, many large earthquakes have occurred in Central and East Java, such as the 1994 large subduction thrust earthquake (Mw 7.6) that produced a tsunami in Banyuwangi. This earthquake was caused by slip over a subducting seamount, which is a locked patch within a decoupled subduction zone (Abercrombie et al., 2001). Another event, the 2006 Yogyakarta earthquake (Mw 6.3), occurred on the inland Opak Fault; the geometry of which has been subsequently determined by SAR interferometry (Tsuji et al., 2009). There have also been other historical earthquakes (M>6) along the Sunda Arc dating from the 1900s that have been documented by Newcomb and McCann (1987).

Previous studies have evaluated the seismicity in the study area using the Agency for Meteorology, Climatology, and Geophysics of Indonesia (BMKG) regional network. These include: hypocenter determination using a non-linear method in West Java (Rosalia et al., 2017) and in Central and East Java (Muttaqy et al., 2019); hypocenter relocation using a double-difference method in West Java (Supendi et al., 2018), and in East Java (Cahyaningrum et al.,

2015); and teleseismic double-difference along the Sunda Arc (Nugraha et al., 2018). Many local seismic networks have been deployed and have also contributed to seismicity and tomography studies in Central and East Java. These include: the DOMERAPI network that was used to comprehensively study the crustal structure beneath the Merapi volcano (Ramdhan et al., 2015, 2016, 2017a, b, 2019); the MERAMEX network, consisting of onshore and offshore seismographic stations in Central Java, that successfully determined the crustal and upper mantle structure beneath Central and East Java; as well as studies related to volcanic activities in the study area (Koulakov et al. 2007, 2009; Wagner et al. 2007; Rohadi et al. 2013; Bohm et al. 2013; Zulfakriza et al. 2014; Haberland et al. 2014; Wölbern and Rümpker 2016); and ambient noise tomography, using both the BMKG network and portable seismographs in East Java (Martha et al., 2017).

Central and East Java are considered to be the most densely populated region in Indonesia; over 73 million people live in this highly seismic area (Central Bureau of Statistics of Indonesia (BPS), 2012). Due to the potential of high seismic hazard, the investigation of earthquake clusters in this region is essential in order to improve and support the Indonesian seismic hazard map. Therefore, this study aims to determine precise hypocenter locations and analyze the pattern of seismic distribution in Central and East Java.

2 Data and Method

We manually re-picked P- and S-arrivals on waveforms recorded at 34 BMKG stations in Central and East Java (Fig 1) in the period January 2009 to September 2017, using Seisgram2K

(Lomax and Michelini, 2009). The following criteria were used for selecting events for determining the hypocenters: (i) recorded by at least four stations and having clear onset P-and S-arrival times, and (ii) having magnitude (Mw) > 3 (Fig 2a). To assure quality control during the picking process, we plotted a Wadati Diagram to independently check the linear relationship between phase data (Fig 2b); a Vp/Vs ratio of 1.75 was obtained. The hypocenter locations were determined using a non-linear method in the NLLoc program (Lomax et al., 2000) with the global 1-D seismic velocity model AK135 (Kennett et al.,1995). This method uses the oct-tree importance sampling to produce an estimation of the posterior density function (PDF) for the hypocenter location in 3D. A similar method was implemented to determine hypocenters in West Java (Rosalia et al., 2017), as well as in doing an aftershock analysis of the May 27, 2006, M 6.4 Yogyakarta earthquake (Husni et al., 2018; Wulandari et al., 2018); it was also used in the Pannonian Basin in Hungary (Wéber and Süle, 2014), the Central-Eastern Alps of North Italy (Viganò et al., 2015), and the eastern border faults of the Main Ethiopian Rift (Lapins et al., 2020), among many others.

In order to have a more reliable seismic velocity model of the area beneath the study area, we updated the 1-D seismic velocity model from VELEST code which simultaneously inverts the hypocenter, velocity and station corrections. The code performs an iterative damped least-squares inversion where each iteration solves ray tracing and inverse problems. We applied the damping to control which parameters of earthquake locations, layer velocities, and station corrections needed to be adjusted. The higher the damping value, the fewer parameters are allowed to vary in the inversion process (Kissling, 1995). In this study, we selected events that

have a maximum azimuthal gap of 180^{o} to assure that the events are well localized by the seismograph network and are representative of the subsurface information in the study area. The 1-D priori seismic velocity model considered for this study was taken from Koulakov et al. (2007) as it successfully defined crustal and upper mantle P-average velocity (Vp) beneath Central Java and combined well with the global AK135 model (Kennett et al., 1995) for the deeper part of the structure (> 210 km). We used the Vp/Vs ratio of 1.75 derived by using a Wadati Diagram to scale the initial Vs model. We then randomly generated 10 initial velocity models that were uniformly distributed within ±20% relative to the priori model.

We then ran the HypoDD program (Waldhauser, 2001), which implements the double-difference algorithm (Waldhauser and Ellsworth, 2000), to relocate earthquakes that had previously been determined using the non-linear method. The double-difference algorithm is based on the assumption that if the distance between two earthquakes is smaller than their distances to the station and the length scale of the structure, then the ray paths of these earthquakes are similar. HypoDD can minimize the residuals between observed and calculated travel-time differences for pairs of earthquakes recorded at the same station. Thus, the errors due to an inaccurate velocity model can be minimized without using station corrections.

In addition to double-difference relocation, we also used waveform cross-correlation (WCC) data to obtain more reliable relative travel time data. Using waveform cross-correlation data minimizes the error commonly associated with the arrival-time picking process (Hauksson and Shearer, 2005; Schaff and Waldhauser, 2005). This process relies on the similarity between

waveforms recorded at the same station. The WCC technique is initially performed by selecting the seismogram with the highest signal-to-noise ratio (SNR) to be the master event of each earthquake cluster as determined by a double-difference algorithm. We assumed that the onsets of P- and S-waves on a highly SNR seismogram were clear enough to be identified. The other seismograms at the same cluster and the same station were cross-correlated and the picked arrival times were refined to the shifted time. Cross-correlation has been widely used, in addition to the double-difference algorithm, to relocate hypocenters; e.g., Sumatra (Pesicek et al., 2010; Waldhauser et al., 2012; Muksin et al., 2014), Central Java (Sipayung et al., 2018), the Nicoya Peninsula in Costa Rica (Hansen et al., 2006), the 2019 Ridgecrest earthquake sequence in eastern California (Lin, 2020), the Alboran slab of the westernmost part of the Mediterranean Sea (Sun and Bezada, 2020), among others.

3 Results and Discussions

The hypocenter determination results consisted of the location of 1,529 events, using 11,192 phases for each P and S-wave (Fig 3). To quantify the capability of the BMKG network in detecting earthquakes, we plotted both the cumulative number of earthquakes and the frequency-magnitude relationship in the time period 2009 to 2017 using the maximum likelihood method, which was applied in the Zmap package (Wiemer, 2001). The regional BMKG network has a 3.4 magnitude of completeness (Mc), with many more earthquakes that could still be recorded; as compared to global networks such as USGS, which has a Mc of 4.2 with fewer earthquakes that could be recorded (Fig 4).

We conducted the updated 1-D seismic velocity model by employing the selected 154 located events that have a maximum azimuthal gap of 180^{o} and which were expected to represent the average velocity of Central and East Java. This is a trial-and-error process done by defining various initial models and parameters, iteratively. For each initial model, we used various velocity dampings from 0.1 to 1.0, while the hypocenter and station correction dampings were set to 0.01 and 0.1, respectively. This resulted in 100 1-D seismic velocity model solutions for each Vp and Vs. We selected 1 out of 100 updated models that was considered to be the best solution having minimal residual (Fig 5).

Several earthquakes that may be generated by the same source mechanism will produce high waveform similarity at a common station. Therefore, the waveform cross-correlation (WCC) process ensures the consistency of P and S-wave phase identification. We computed the cross-correlation functions for P-and S-waves using a time window of 0.2 s before and 2 s after the onset of P-arrival time and 1.4 s before and 5 s after S-arrival time onset. We used the Butterworth filter between 1-6 Hz and coefficient correlation criteria that are greater than 0.7. Figure 6 shows an example of the cross-correlation results at RTBI and PWJI stations. The output of the WCC process that was saved as input for HypoDD was the lag time and coefficient correlation. We also used this technique to estimate the uncertainty of observed data, resulting in the average of picking errors for P- and S-arrivals as 0.1886 s and 0.297 s, respectively.

We applied both catalog and cross-correlation differential time data in HypoDD to improve the quality of event clustering. The weighting of the distance between paired events for catalog data (WDCT) was set to 45 km in the first four iterations; it was then set to 15 km and 35 km for correlation data (WDCC) in the second four iterations. These parameters are distance cutoff parameters used in HypoDD to remove data for event pairs with separation distances larger than the given values (Waldhauser, 2001). The selection of the optimum damping factor depends on the system conditions to be resolved, which is represented as the condition number (CND) (Hauksson and Shearer, 2005). We used the damping factors of 85 and 70, resulting in a condition number between 40 and 80.

As a result, we were successful in relocating 1,127 out of 1,529 events in the Central and East Java region (Table S1 in the supplementary material) that form more of a cluster in several areas than the initial locations indicated (Fig 7). The average shifting of earthquake locations in X (east-west), Y (north-south), and Z (depth) directions are 3.37, 4.76, and 10.4 km, respectively; with the maximum shifted locations being 29.2, 44.36, and 49.98 km, respectively (Fig S1). This somewhat significant improvement was also statistically proven by the histogram of residual times (Fig 8) which had standard deviations of 0.912, 0.476, and 0.402 s^2 before relocation, after relocation without, and with WCC, respectively. The distribution of location errors in X, Y and Z directions are also provided in Figure S2.

Based on the relocation results, the seismicity in Central and East Java are predominantly distributed in the south of Java Island. The vertical cross-section of blocks B-F (Fig 9) shows

197 subduction-related events that are compatible with the slab 1.0 model (Hayes et al., 2012). The
198 dipping angle of the slab steepens from west to east. Each block represents several interesting
199 clusters in the study area, such as the Kebumen, Yogyakarta, Pacitan, Malang, and Banyuwangi
200 clusters.
201
202 Block B contains the Kebumen cluster where the Mw 6.2 Kebumen earthquake occurred on
203 January 25, 2014 (Fig 9). The focal mechanism of the Global Centroid Moment Tensor
204 (GCMT) (Dziewonski et al., 1981; Ekström et al., 2012) (https://www.globalcmt.org/), shows
205 a normal faulting mechanism, while the surrounding events in the cluster are dominated by a
206 thrusting mechanism (Fig 12). Based on the location and focus depth, the seismicity in this
207 cluster consists of intraslab events associated with an intense deformation zone due to plate
208 collision (Serhalawan et al., 2017).
209
210 The vertical cross-sections of blocks C, D, and E depict the Yogyakarta, Pacitan, and Malang
211 clusters, respectively (Fig 9). These seismic clusters are located at the forearc of the Java
212 subduction system and are dominated by subduction-related events with thrusting mechanisms
213 and normal-faulting mechanisms in certain areas, based on the GCMT focal mechanism (Fig
214 12). The steeper angle of the slab causes an increase in the number of earthquakes towards the
215 east with depths of up to 200 km. On April 10, 2021, a Mw 6.1 earthquake with a thrusting
216 fault mechanism occurred near the Malang cluster. The event produced strong shaking with
217 MMI V in East Java (http://shakemap.bmkg.go.id/), causing fatalities and damage to buildings.
218 Block F represents an interesting cluster in the south of Banyuwangi, close to the location of

the Mw 7.8 Banyuwangi earthquake that occurred in 1994 (Fig 9). The seismicity in this area is most likely related to the subducting plate behind seamount which triggered the normal faulting earthquake at the outer rise of the Indo-Australian Plate (Abercrombie et al., 2001) (Fig 12).

Additionally, the shallow clustered earthquakes are probably controlled by active inland faults, such as in block A, northern block D and block F, and are associated with the Opak Fault, the Kendeng Thrust Fault, and the Rembang-Madura-Kangean-Sakala (RMKS) Fault Zones, respectively (Fig 9). The Opak Fault is considered be the cause of the 2006 Yogyakarta earthquake (Mw 6.3); the aftershocks of which were still observed in the data during the period of our study. The geometry of the Opak Fault is still debatable, whether the fault plane is east- or west-dipping. Based on the vertical cross-section of block A, the relocated events are clustered in the east of the Opak Fault lineament with depths between 5-20 km, indicating that the fault plane is more likely east-dipping. Based on SAR interferometry observations, it was concluded that the geometry of the Opak Fault is considered to be an east-dipping left-lateral fault which ensures that the hypocenter distribution is in the eastern part of the fault (Tsuji et al., 2009). Several previous studies also support this result and show that the aftershock distribution of the 2006 Yogyakarta earthquake is parallel to the Opak Fault lineament and located 5-10 km to the east (Husni et al., 2018; Wulandari et al., 2018). Furthermore, a recent crustal deformation study suggests that the distribution of these aftershocks is most likely related to the activity of unmapped local faults, instead of the Opak Fault, which are currently

accumulating stress in Yogyakarta as the results of an ongoing postseismic deformation of the 2006 Yogyakarta earthquake (Widjajanti et al., 2020).

Furthermore, shallow clustered events at depths of less than 30 km were observed in the northern part of block D, suggesting activity in the Kendeng Thrust Zone (Figs 9 and 10). This is a major fault zone in the study area; it extends for 200 km from Central to East Java and is an accumulation of thrusts and folds (Pusat Studi Gempa Nasional (PuSGeN), 2017). Evidence of movement in this fault can be observed by the presence of uplifted alluvial terrace along with this fault's activity (Marliyani, 2016). Based on their geodetic study, Koulali et al. (2017) estimate the average slip rate of Kendeng Thrust Fault to be about 2.3-4.1 mm/yr. However, whether the seismicity is controlled by the local fault or by volcanic activity of Mt. Pandan and Mt. Wilis is still debatable. In 2015, an earthquake in Madiun (Mw 4.2) caused damage to several houses due to its shallow depth and the amplification effect in the north of Mt. Pandan (Nugraha et al., 2016). Previous studies suggest that this event may be related to the local strike-slip fault (Nugraha et al., 2016; Sipayung et al., 2018). In contrast, a gravity survey that was conducted around Mt. Pandan indicated that a low-density anomaly, possibly related to hot material or a magma body, may have triggered the seismicity (Santoso et al., 2018). The survey suggests that the subduction process resulted in fault movement which triggered a magma flow to the surface at the same time. Thus, we conclude that the seismicity in this cluster might be associated with both Kendeng Thrust activity and a magmatic process.

There is a shallow seismic cluster around Rembang and Madura in the northern part of East Java (Fig 11) which most likely corresponds to the Rembang-Madura-Kangean-Sakala (RMKS) Fault Zone. We suggest that this fault extends to the north of Surabaya where shallow events are observed. Recent destructive earthquakes have occurred in the RMKS Fault Zone, i.e., the Madura earthquake (Mw 4.3) and the Situbondo earthquake (Mw 6.3), both in 2018 but with different mechanisms. The Madura earthquake (Mw 4.3) was more likely related to the strike-slip RMKS Fault, while the Situbondo earthquake (Mw 6.3) has a thrusting mechanism based on the GCMT focal mechanism solution (Fig 12). This suggests that the Situbondo earthquake had a strong connection with the Back Arc Thrust that may extend from the east.

Several other active inland faults may control the seismicity in the Central and East Java region, for example, the Pasuruan Fault, the Lasem Fault, the Muria Fault, the Semarang Thrust Fault, and the Probolinggo Fault. These have not shown a significant number of earthquakes during the time period of 2009 to 2017. Hence, “unpaired” events that are not clustered beyond distance weighting were eliminated by the double-difference algorithm. Moreover, earthquakes associated with volcanic activities were also not well-determined due to the limited seismograph network used in this study.

4 Conclusions

We have successfully determined 1,529 earthquakes in the Central and East Java region in the time period of January 2009 to September 2017, using a manual re-picking process. We then

283 relocated 1,127 events by applying waveform cross-correlation data in the double-difference
284 algorithm. Overall, our results show that the seismic pattern in Central and East Java is
285 predominantly distributed in the south of Java Island, such as the Kebumen, Yogyakarta,
286 Pacitan, Malang, and Banyuwangi clusters. These seismic clusters are subduction-related
287 events that are compatible with the slab 1.0 model (Hayes et al., 2012). The dipping angle of
288 the slab steepens to the east, causing an increase towards the east in the number of earthquakes
289 with depths of up to 200 km.
290
291 Shallow clustered earthquakes in the mainland of the Central and East Java region were also
292 observed; these correspond to active inland faults that include the Opak Fault, the Kendeng
293 Thrust Fault, and the Rembang-Madura-Kangean-Sakala (RMKS) Fault Zone. Based on the
294 relocation results, the seismicity around the Opak Fault indicates east-dipping geometry, since
295 the relocated events were distributed to the east of the Opak Fault lineament at depths between
296 5-20 km. Meanwhile, the shallow seismic cluster (< 30 km depths) around the Kendeng Thrust
297 Fault in the north of Madiun coincide with volcanoes present there, suggesting that these are
298 triggered by both active local faults and magmatic processes beneath Mt. Pandan and Mt. Wilis.
299 We suggest that the RMKS Fault in the northern part of East Java extends to the north of
300 Surabaya where shallow events are observed. Several other active inland faults have not shown
301 significant seismicity, and earthquakes caused by volcanic activities were not well-determined
302 by the seismic network used in this study.
303
304 **Authors' contributions**

FM, ADN, NTP, SR, PS conceived the study; FM, ADN, DPS, ZZ contributed to the writing of the manuscript. All authors contributed to the preparation of the manuscript. All authors have read and approved the final manuscript.

Acknowledgements

We are grateful to the Agency for Meteorology, Climatology, and Geophysics (BMKG) Indonesia for providing waveform and catalog data. All figures in this study were made by using the Generic Mapping Tools developed by Paul Wessel and Walter H.F. Smith.

Competing interests

We declare that we have no significant competing financial, professional or personal interests that might have influenced the performance or presentation of the work described in this manuscript.

Availability of data and materials

The datasets supporting the conclusions of this article are included within the article and its additional files.

Funding

This study was supported by the PMDSU 2017 scholarship from the Ministry of Research, Technology, and Higher Education of the Republic of Indonesia, awarded to FM. It was also

partially supported by PUPT 2016 and 2017 from the Ministry of Research, Technology, and Higher Education of the Republic of Indonesia, awarded to ADN.

References

Abercrombie RE, Antolik M, Felzer K, Ekstrom G (2001) The 1994 Java tsunami earthquake : Slip over a subducting seamount. Journal of Geophysical Research 106:6595–6607. https://doi.org/10.1029/2000JB900403

Bohm M, Haberland C, Asch G (2013) Imaging fluid-related subduction processes beneath Central Java (Indonesia) using seismic attenuation tomography. Tectonophysics 590:175–188. https://doi.org/10.1016/J.TECTO.2013.01.021

Cahyaningrum AP, Nugraha AD, Puspito NT (2015) Earthquake hypocenter relocation using double difference method in East Java and surrounding areas. AIP Conference Proceedings 1658:. https://doi.org/10.1063/1.4915029

Central Bureau of Statistics of Indonesia (BPS) (2012) Penduduk Indonesia menurut Provinsi 1971, 1980, 1995, 2000 dan 2010

Dziewonski AM, Chou TA, Woodhouse JH (1981) Determination of earthquake source parameters from waveform data for studies of global and regional seismicity. Journal of Geophysical Research 86:2825–2852. https://doi.org/10.1029/JB086iB04p02825

Ekström G, Nettles M, Dziewoński AM (2012) The global CMT project 2004-2010: Centroid-moment tensors for 13,017 earthquakes. Physics of the Earth and Planetary Interiors 200–201:1–9. https://doi.org/10.1016/j.pepi.2012.04.002

Haberland C, Bohm M, Asch G (2014) Accretionary nature of the crust of Central and East Java (Indonesia) revealed by local earthquake travel-time tomography. Journal of Asian Earth Sciences 96:287–295. https://doi.org/10.1016/J.JSEAES.2014.09.019

Hansen SE, Schwartz SY, DeShon HR, González V (2006) Earthquake relocation and focal mechanism determination using waveform cross correlation, Nicoya Peninsula, Costa Rica. Bulletin of the Seismological Society of America 96:1003–1011. https://doi.org/10.1785/0120050129

Hauksson E, Shearer P (2005) Southern California hypocenter relocation with waveform cross-correlation, part 1: Results using the double-difference method. Bulletin of the Seismological Society of America 95:896–903. https://doi.org/10.1785/0120040167

Hayes GP, Wald DJ, Johnson RL (2012) Slab1.0: A three-dimensional model of global subduction zone geometries. Journal of Geophysical Research: Solid Earth 117:1–15. https://doi.org/10.1029/2011JB008524

Husni YM, Nugraha AD, Rosalia S, et al (2018) Aftershock location determination of the 27 May 2006, M 6.4 Yogyakarta earthquake using a non-linear algorithm: A preliminary results. AIP Conference 020049:020049–020049. https://doi.org/10.1063/1.5047334

Kennett BLN, Engdahl ER, Buland R (1995) Constraints on seismic velocities in the Earth from travel times. Geophysical Journal International 122:108–124. https://doi.org/10.1111/j.1365-246X.1995.tb03540.x

Koulakov I, Bohm M, Asch G, et al (2007) P and S velocity structure of the crust and the upper mantle beneath central Java from local tomography inversion. Journal of Geophysical Research: Solid Earth 112:1–19. https://doi.org/10.1029/2006JB004712

Koulakov I, Jakovlev A, Luehr BG (2009) Anisotropic structure beneath central Java from local earthquake tomography. Geochemistry Geophyscs Geosystems 10:. https://doi.org/10.1029/2008GC002109

Koulali A, McClusky S, Susilo S, et al (2017) The kinematics of crustal deformation in Java from GPS observations: Implications for fault slip partitioning. Earth and Planetary Science Letters 458:69–79. https://doi.org/10.1016/j.epsl.2016.10.039

Lapins S, Kendall JM, Ayele A, et al (2020) Lower-Crustal Seismicity on the Eastern Border Faults of the Main Ethiopian Rift. Journal of Geophysical Research: Solid Earth 125:0–2. https://doi.org/10.1029/2020jb020030

Lin G (2020) Waveform cross-correlation relocation and focal mechanisms for the 2019 ridgecrest earthquake sequence. Seismological Research Letters 91:2055–2061. https://doi.org/10.1785/0220190277

Lomax A, Michelini A (2009) M wpd : a duration – amplitude procedure for rapid determination of earthquake magnitude and tsunamigenic potential from P waveforms. Geophysical Journal International 176:200–214. https://doi.org/10.1111/j.1365-246X.2008.03974.x

Lomax A, Virieux J, Volant P, Berge-Thierry C (2000) Probabilistic Earthquake Location in 3D and Layered Models BT - Advances in Seismic Event Location. In: Thurber CH, Rabinowitz N (eds) Advances in Seismic Event Location. Modern Approches in Geophysics. Springer Netherlands, Dordrecht, pp 101–134

389 Malod JA, Karta K, Beslier MO, Zen MT (1995) From normal to oblique subduction:
390 Tectonic relationships between Java and Sumatra. Journal of Southeast Asian Earth
391 Sciences 12:85–93. https://doi.org/10.1016/0743-9547(95)00023-2

392 Marliyani GI (2016) Neotectonics of Java, Indonesia: Crustal Deformation in the Overriding
393 Plate of an Orthogonal Subduction System

394 Martha AA, Cummins P, Saygin E, Widiyantoro S (2017) Imaging of upper crustal structure
395 beneath East Java – Bali , Indonesia with ambient noise tomography. Geoscience
396 Letters. https://doi.org/10.1186/s40562-017-0080-9

397 Muksin U, Haberland C, Nukman M, et al (2014) Journal of Asian Earth Sciences Detailed
398 fault structure of the Tarutung Pull-Apart Basin in Sumatra , Indonesia , derived from
399 local earthquake data. Journal of Asian Earth Sciences 96:123–131.
400 https://doi.org/10.1016/j.jseaes.2014.09.009

401 Muttaqy F, Nugraha AD, Puspito NT, Supendi P (2019) A Non-Linear Method for
402 Hypocenter Determination around Central and East Java Region : Preliminary Result.
403 IOP Conference Series: Earth and Environmental Science 318:012008–012008.
404 https://doi.org/10.1088/1755-1315/318/1/012008

405 Newcomb KR, Mccann WR (1987) Seismic History and Seismotectonics of The Sunda Arc.
406 Journal of Geophysical Research 92:421–439.
407 https://doi.org/10.1029/JB092iB01p00421

408 Nugraha AD, Shiddiqi HA, Widiyantoro S, et al (2018) Hypocenter Relocation along the
409 Sunda Arc in Indonesia , Using a 3D Seismic-Velocity Model. Seismological
410 Research Letters 89:603–612. https://doi.org/10.1785/0220170107

411 Nugraha AD, Supendi P, Shiddiqi HA, Widiyantoro S (2016) Unexpected earthquake of June
412 25th, 2015 in Madiun, East Java. AIP Conference Proceedings 1730:.
413 https://doi.org/10.1063/1.4947369

414 Pesicek JD, Thurber CH, Zhang H, et al (2010) Teleseismic double - difference relocation of
415 earthquakes along the Sumatra - Andaman subduction zone using a 3 - D model.
416 Journal of G 115:1–20. https://doi.org/10.1029/2010JB007443

417 Pusat Studi Gempa Nasional (PuSGeN) (2017) Peta Sumber dan Bahaya Gempa Indonesia
418 Tahun 2017, First. Pusat Penelitian dan Pengembangan Perumahan dan Pemukiman
419 Badan Penelitian dan Pengembangan Kementerian Pekerjaan Umum dan Perumahan
420 Rakyat, Bandung

421 Ramdhan M, Nugraha AD, Widiyantoro S, et al (2016) Observation of Seismicity Based on
422 DOMERAPI and BMKG Seismic Networks : A Preliminary Result from

DOMERAPI Project. AIP Conference Proceedings 1730:1–8. https://doi.org/10.1063/1.4947377

Ramdhan M, Nugraha AD, Widiyantoro S, Valencia AA (2015) Earthquake Location Determination Using Data from DOMERAPI and BMKG Seismic Networks : A Preliminary Result of DOMERAPI Project. AIP Conference Proceedings 1658:1–5. https://doi.org/10.1063/1.4915015

Ramdhan M, Widiyantoro S, Nugraha AD, et al (2019) Detailed seismic imaging of Merapi volcano, Indonesia, from local earthquake travel-time tomography. Journal of Asian Earth Sciences 177:134–145. https://doi.org/10.1016/j.jseaes.2019.03.018

Ramdhan M, Widiyantoro S, Nugraha AD, et al (2017a) Seismic Travel-time Tomography beneath Merapi Volcano and its Surroundings : A Preliminary Result from DOMERAPI Project. IOP Conference Series: Earth and Environmental Science 62:. https://doi.org/10.1088/1755-1315/62/1/012039

Ramdhan M, Widiyantoro S, Nugraha AD, et al (2017b) Relocation of hypocenters from DOMERAPI and BMKG networks : a preliminary result from DOMERAPI project. Earthquake Science 30:67–79. https://doi.org/10.1007/s11589-017-0178-3

Rohadi S, Widiyantoro S, Nugraha AD, Masturyono (2013) Tomographic Imaging of P- and S-wave Velocity Structure Beneath Central Java , Indonesia : Joint Inversion of the MERAMEX and MCGA Earthquake Data. International Journal of Tomography and Simulation 24:16–16

Rosalia S, Widiyantoro S, Dian Nugraha A, et al (2017) Hypocenter Determination Using a Non-Linear Method for Events in West Java, Indonesia: A Preliminary Result. IOP Conference Series: Earth and Environmental Science 62:. https://doi.org/10.1088/1755-1315/62/1/012052

Santoso D, Wahyudi EJ, Alawiyah S, et al (2018) Gravity Structure around Mt . Pandan , Madiun , East Java , Indonesia and Its Relationship to 2016 Seismic Activity. Open Geosciences 10:882–888. https://doi.org/10.1515/geo-2018-0069

Schaff DP, Waldhauser F (2005) Waveform cross-correlation-based differential travel-time measurements at the northern California seismic network. Bulletin of the Seismological Society of America 95:2446–2461. https://doi.org/10.1785/0120040221

Serhalawan YR, Sianipar D, Suardi I (2017) The January 25 th , 2014 Kebumen Earthquake : A Normal Faulting in Subduction Zone of Southern Java. AIP Conference Proceedings 030002: https://doi.org/10.1063/1.4987061

457 Sipayung R, Alhafiz MR, Agus R, Sianipar D (2018) Relocation of the February 2016 Mt.
458 Pandan earthquake sequence using double difference with waveform cross
459 correlation. AIP Conference Proceedings 020036:020036–020036.
460 https://doi.org/10.1063/1.5047321

461 Sun M, Bezada M (2020) Seismogenic Necking During Slab Detachment: Evidence From
462 Relocation of Intermediate-Depth Seismicity in the Alboran Slab. Journal of
463 Geophysical Research: Solid Earth 125:. https://doi.org/10.1029/2019JB017896

464 Supendi P, Nugraha AD, Puspito NT, et al (2018) Identification of active faults in West Java ,
465 Indonesia , based on earthquake hypocenter determination , relocation , and focal
466 mechanism analysis. Geoscience Letters. https://doi.org/10.1186/s40562-018-0130-y

467 Tsuji T, Yamamoto K, Matsuoka T, et al (2009) Earthquake fault of the 26 May 2006
468 Yogyakarta earthquake observed by SAR interferometry. Earth, Planets and Space
469 61:e29--e32. https://doi.org/10.1186/BF03353189

470 Viganò A, Scafidi D, Ranalli G, et al (2015) Earthquake relocations, crustal rheology, and
471 active deformation in the central–eastern Alps (N Italy). Tectonophysics 661:81–98.
472 https://doi.org/10.1016/J.TECTO.2015.08.017

473 Wagner D, Koulakov I, Rabbel W, et al (2007) Joint inversion of active and passive seismic
474 data in Central Java. Geophysical Journal International 170:923–932.
475 https://doi.org/10.1111/j.1365-246X.2007.03435.x

476 Waldhauser F (2001) HypoDD - A Program to Compute Double-Difference Hypocenter
477 Locations by

478 Waldhauser F, Schaff DP, Diehl T, Engdahl ER (2012) Splay faults imaged by fluid-driven
479 aftershocks of the 2004 M w 9 . 2 Sumatra-Andaman earthquake. Geology 40:243–
480 246. https://doi.org/10.1130/G32420.1

481 Wéber Z, Süle B (2014) Source properties of the 29 January 2011 ML 4.5 Oroszlány
482 (Hungary) mainshock and its aftershocks. Bulletin of the Seismological Society of
483 America 104:113–127. https://doi.org/10.1785/0120130152

484 Widiyantoro S, Gunawan E, Muhari A, et al (2020) Implications for megathrust earthquakes
485 and tsunamis from seismic gaps south of Java Indonesia. Scientific Reports 10:1–11.
486 https://doi.org/10.1038/s41598-020-72142-z

487 Widjajanti N, Pratama C, Parseno, et al (2020) Present-day crustal deformation revealed
488 active tectonics in Yogyakarta, Indonesia inferred from GPS observations. Geodesy
489 and Geodynamics 11:135–142. https://doi.org/10.1016/j.geog.2020.02.001

490 Wiemer S (2001) A software package to analyze seismicity: ZMAP. Seismological Research
491 Letters 72:373–382. https://doi.org/10.1785/gssrl.72.3.373

492 Wölbern I, Rümpker G (2016) Crustal thickness beneath Central and East Java (Indonesia)
493 inferred from P receiver functions. Journal of Asian Earth Sciences 115:69–79.
494 https://doi.org/10.1016/J.JSEAES.2015.09.001

495 Wulandari A, Anggraini A, Suryanto W (2018) Hypocenter Analysis of Aftershocks Data of
496 the Mw 6.3, 27 May 2006 Yogyakarta Earthquake Using Oct-Tree Importance
497 Sampling Method. Applied Mechanics and Materials 881:89–97.
498 https://doi.org/10.4028/www.scientific.net/AMM.881.89

499 Zulfakriza Z, Saygin E, Cummins PR, et al (2014) Upper crustal structure of central Java ,
500 Indonesia , from transdimensional seismic ambient noise tomography. Geophysical
501 Journal International 197:630–635. https://doi.org/10.1093/gji/ggu016

502

Figures:

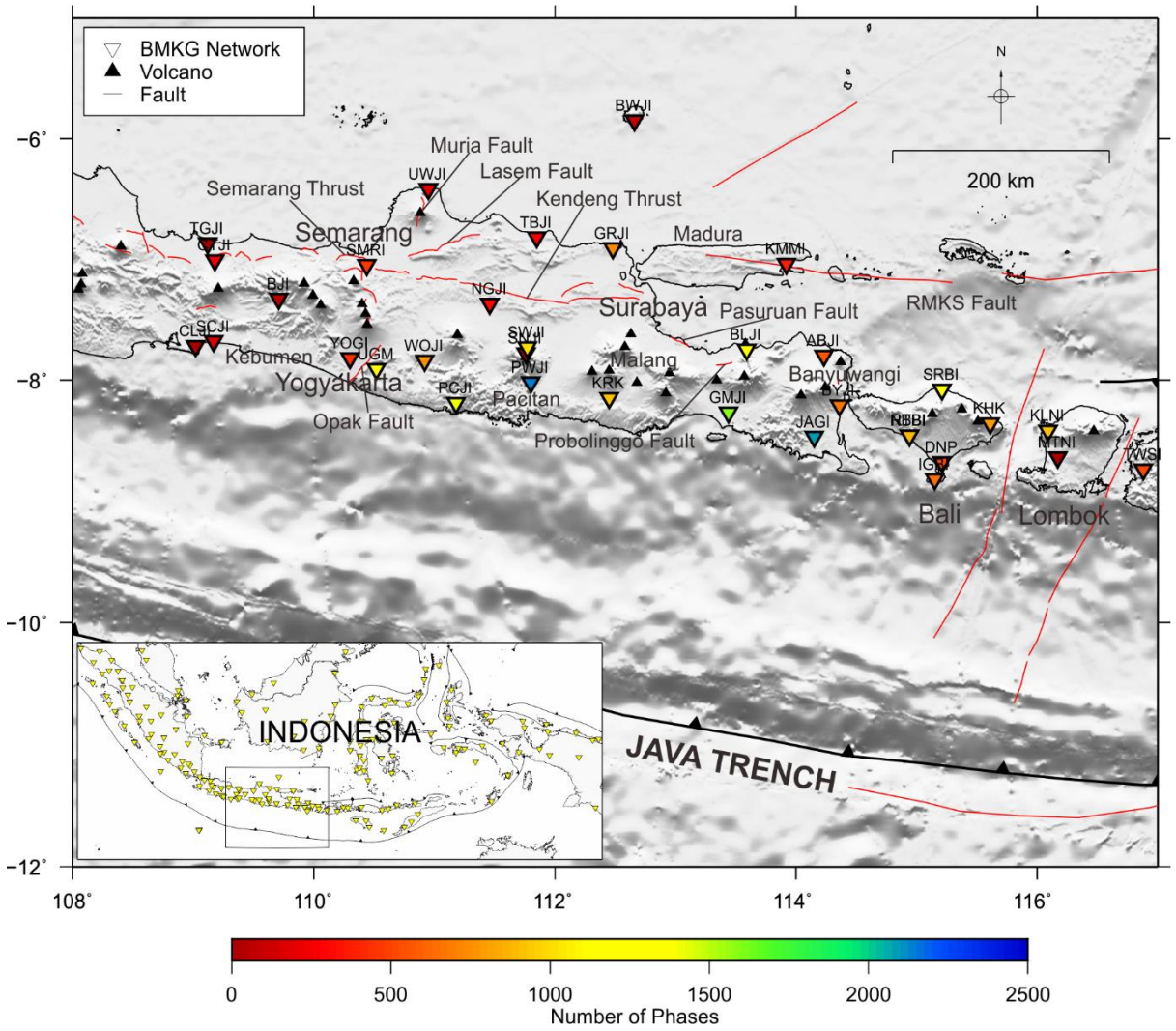

Fig. 1. Map showing the distribution of BMKG seismographic stations (inverted triangles) used in this study, active fault lineament (red lines) and volcanoes (black triangles) (Pusat Studi Gempa Nasional (PuSGeN) 2017). The colors represent the number of phases picked for each station.

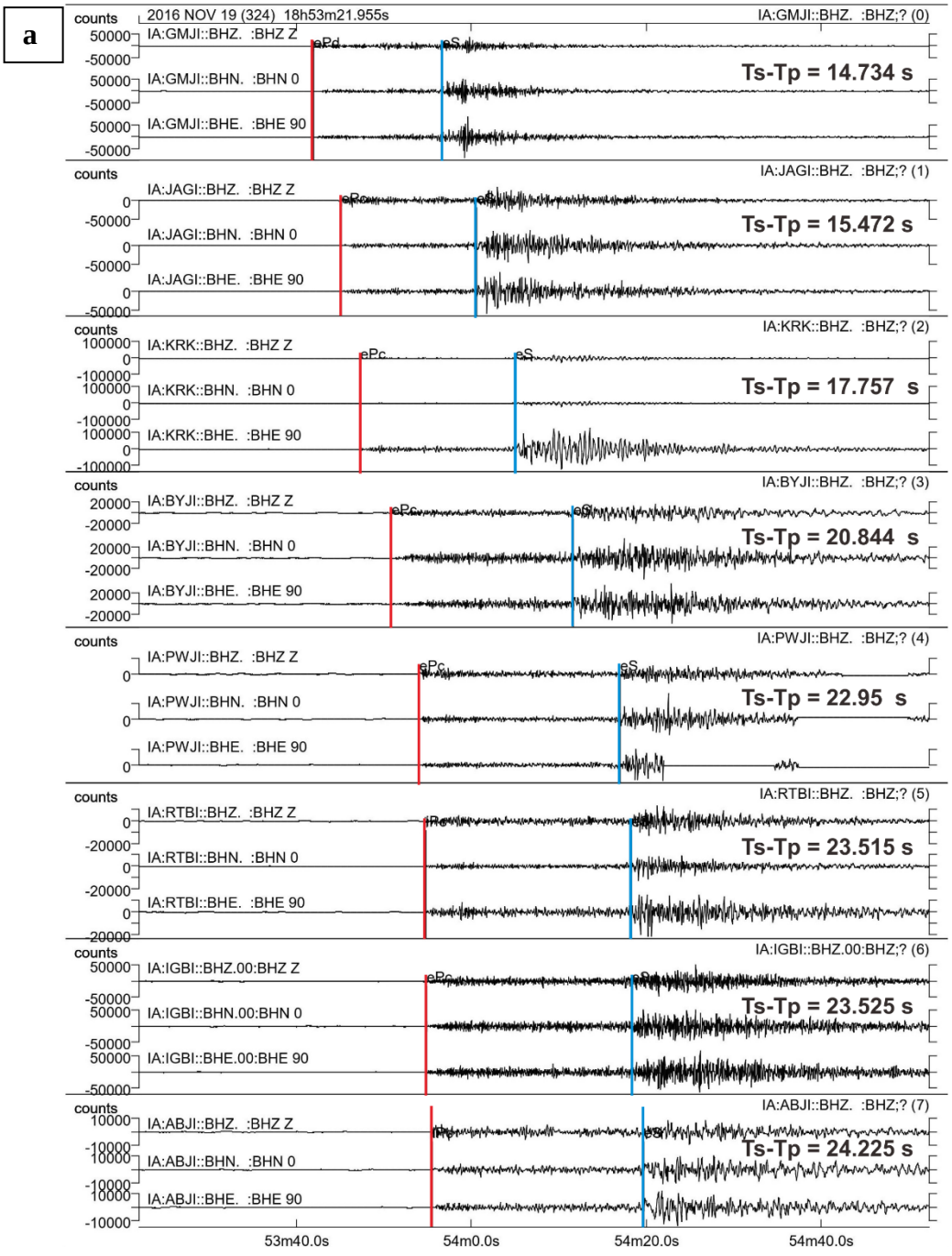
a
counts
2016 NOV 19 (324) 18h53m21.955s
IA:GMJI::BHZ. :BHZ;? (0)
IA:GMJI::BHZ. :BHZ Z
IA:GMJI::BHN. :BHN 0
IA:GMJI::BHE. :BHE 90
ePd
eS
Ts-Tp = 14.734 s
IA:JAGI::BHZ. :BHZ;? (1)
IA:JAGI::BHZ. :BHZ Z
IA:JAGI::BHN. :BHN 0
IA:JAGI::BHE. :BHE 90
ePc
eS
Ts-Tp = 15.472 s
IA:KRK::BHZ. :BHZ;? (2)
IA:KRK::BHZ. :BHZ Z
IA:KRK::BHN. :BHN 0
IA:KRK::BHE. :BHE 90
ePc
eS
Ts-Tp = 17.757 s
IA:BYJI::BHZ. :BHZ;? (3)
IA:BYJI::BHZ. :BHZ Z
IA:BYJI::BHN. :BHN 0
IA:BYJI::BHE. :BHE 90
ePc
eS
Ts-Tp = 20.844 s
IA:PWJI::BHZ. :BHZ;? (4)
IA:PWJI::BHZ. :BHZ Z
IA:PWJI::BHN. :BHN 0
IA:PWJI::BHE. :BHE 90
ePc
eS
Ts-Tp = 22.95 s
IA:RTBI::BHZ. :BHZ;? (5)
IA:RTBI::BHZ. :BHZ Z
IA:RTBI::BHN. :BHN 0
IA:RTBI::BHE. :BHE 90
ePc
eS
Ts-Tp = 23.515 s
IA:IGBI::BHZ.00:BHZ;? (6)
IA:IGBI::BHZ.00:BHZ Z
IA:IGBI::BHN.00:BHN 0
IA:IGBI::BHE.00:BHE 90
ePc
eS
Ts-Tp = 23.525 s
IA:ABJI::BHZ. :BHZ;? (7)
IA:ABJI::BHZ. :BHZ Z
IA:ABJI::BHN. :BHN 0
IA:ABJI::BHE. :BHE 90
ePc
eS
Ts-Tp = 24.225 s
53m40.0s
54m0.0s
54m20.0s
54m40.0s

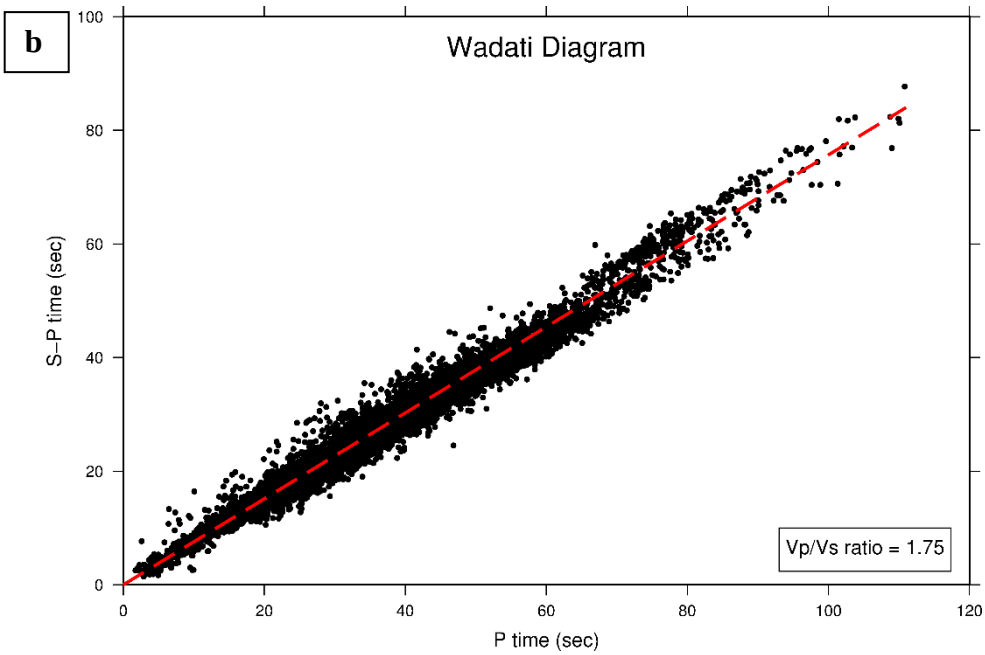

Fig. 2. **a** Three-component seismogram example of a November 19, 2016 event (epicenter location is shown in Fig 3) recorded by the nearest stations (GMJI, JAGI, KRK, BYJI, PWJI, RTBI, IGBI, and ABJI as shown in Fig 1). Red and blue lines indicate the arrival times of P and S-waves, respectively. **b** Wadati Diagram showing a linear relationship between picked phases. The Vp/Vs ratio in this study is 1.75. Red dashed line indicates deviations from a constant Vp/Vs ratio and/or data reading errors.

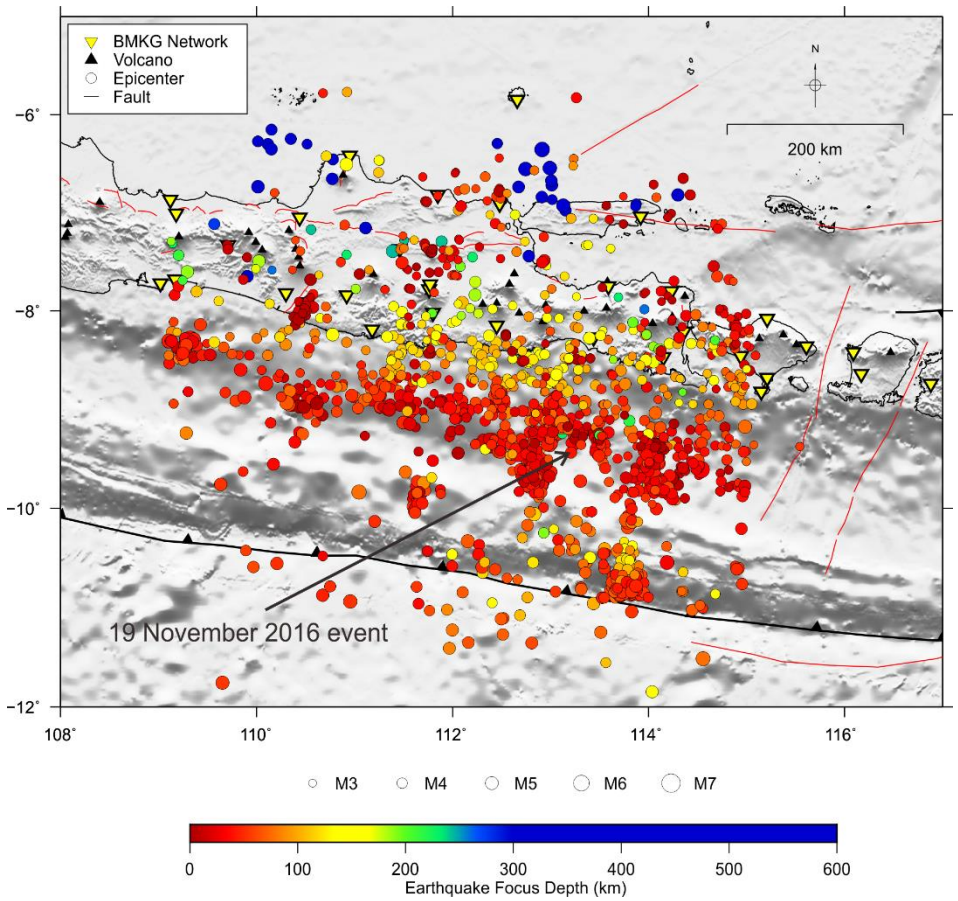

518

519 Fig. 3. Map of seismic distribution determined by this study in the Central and East Java region

520 during the time period 2009 to 2017. The solid-color circles represent earthquake focus depth.

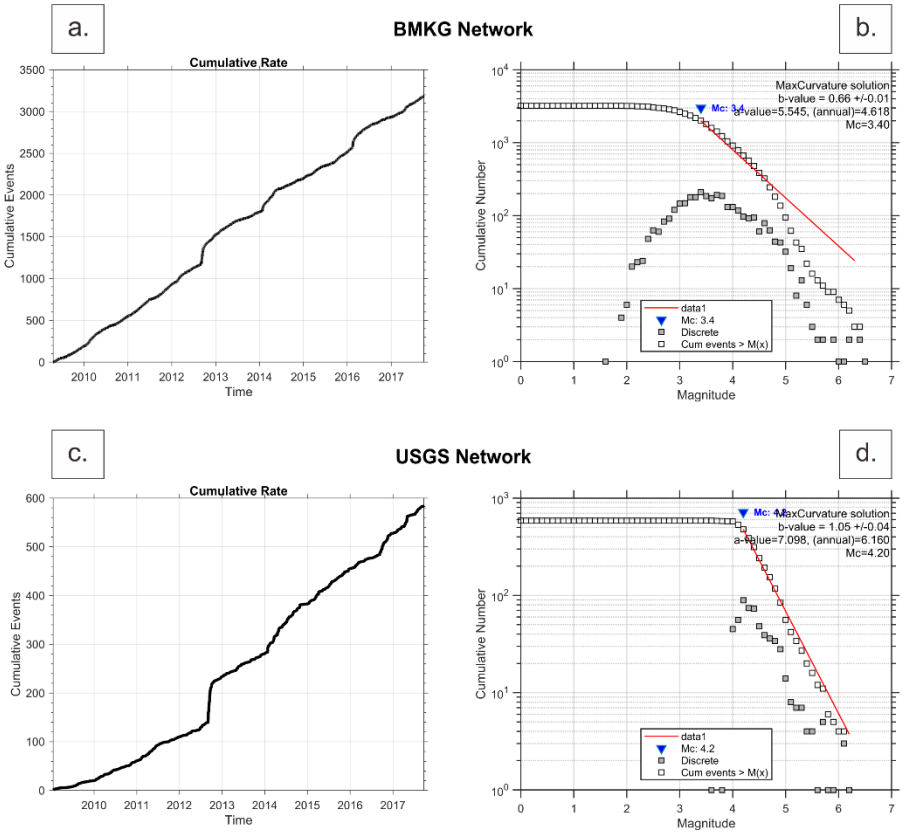

521

522 Fig. 4. **a** Earthquake cumulative numbers and **b** earthquake magnitude-frequency in relation to

523 the regional BMKG network, compared to **c** earthquake cumulative numbers and **d** earthquake

524 magnitude-frequency in relation to the global USGS network.

525

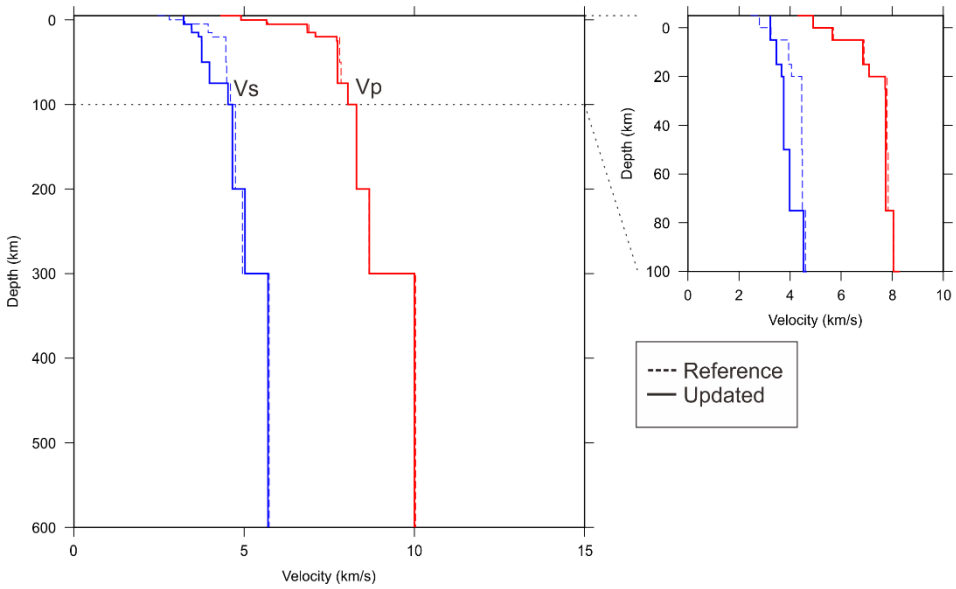

Fig. 5. The updated 1-D seismic velocity model applied to the hypocenter relocation process (bold lines). The red and blue lines indicate Vp and Vs, respectively. The dashed lines reference the 1-D seismic velocity model taken from Koulakov et al. (2007) and the AK135 (Kennett et al.,1995).

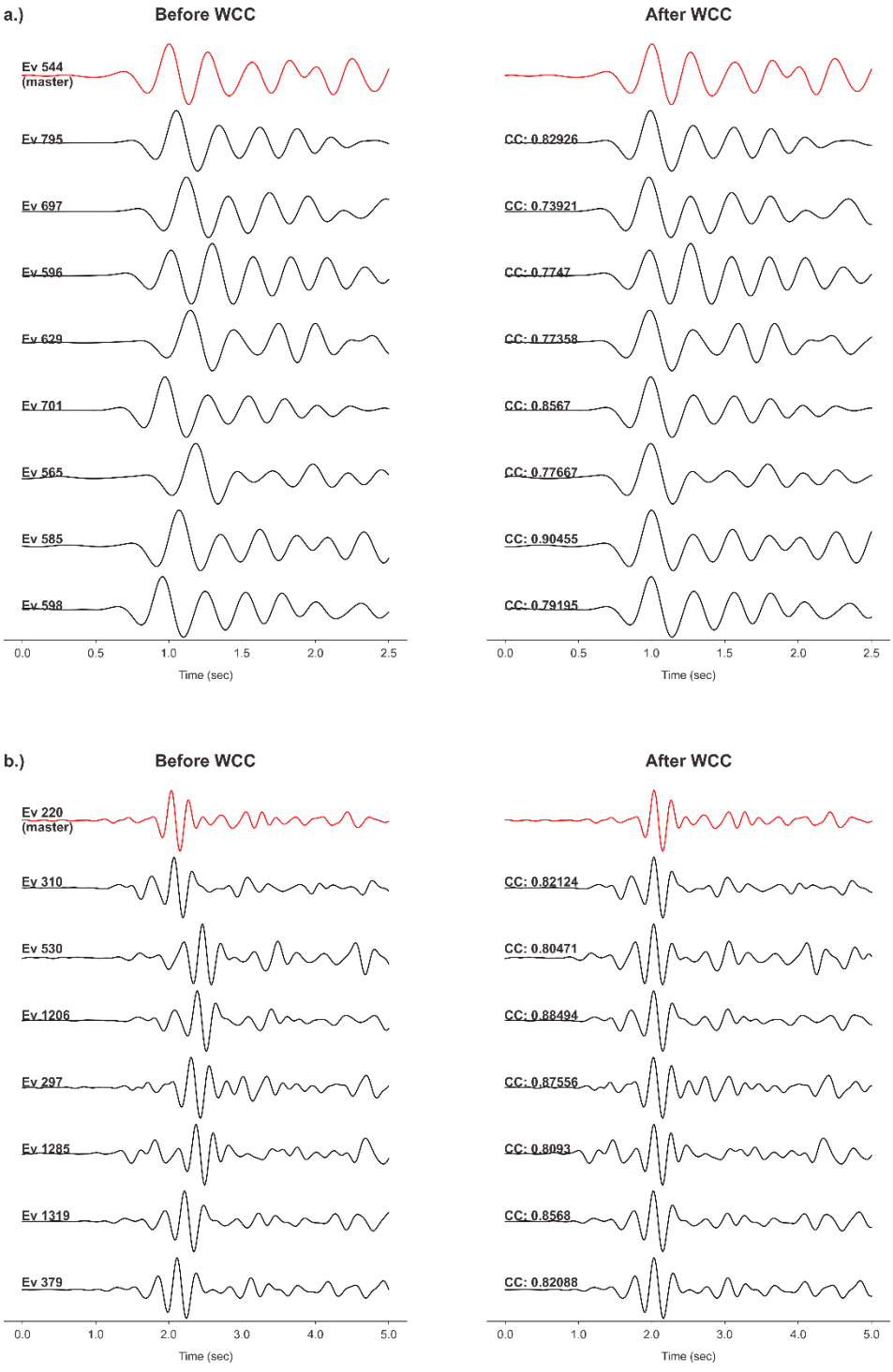

Fig. 6. Example of the waveform cross-correlation (WCC) process for events recorded at common stations. **a** P-waves recorded at RTBI station. **b** S-waves recorded at PWJI station.

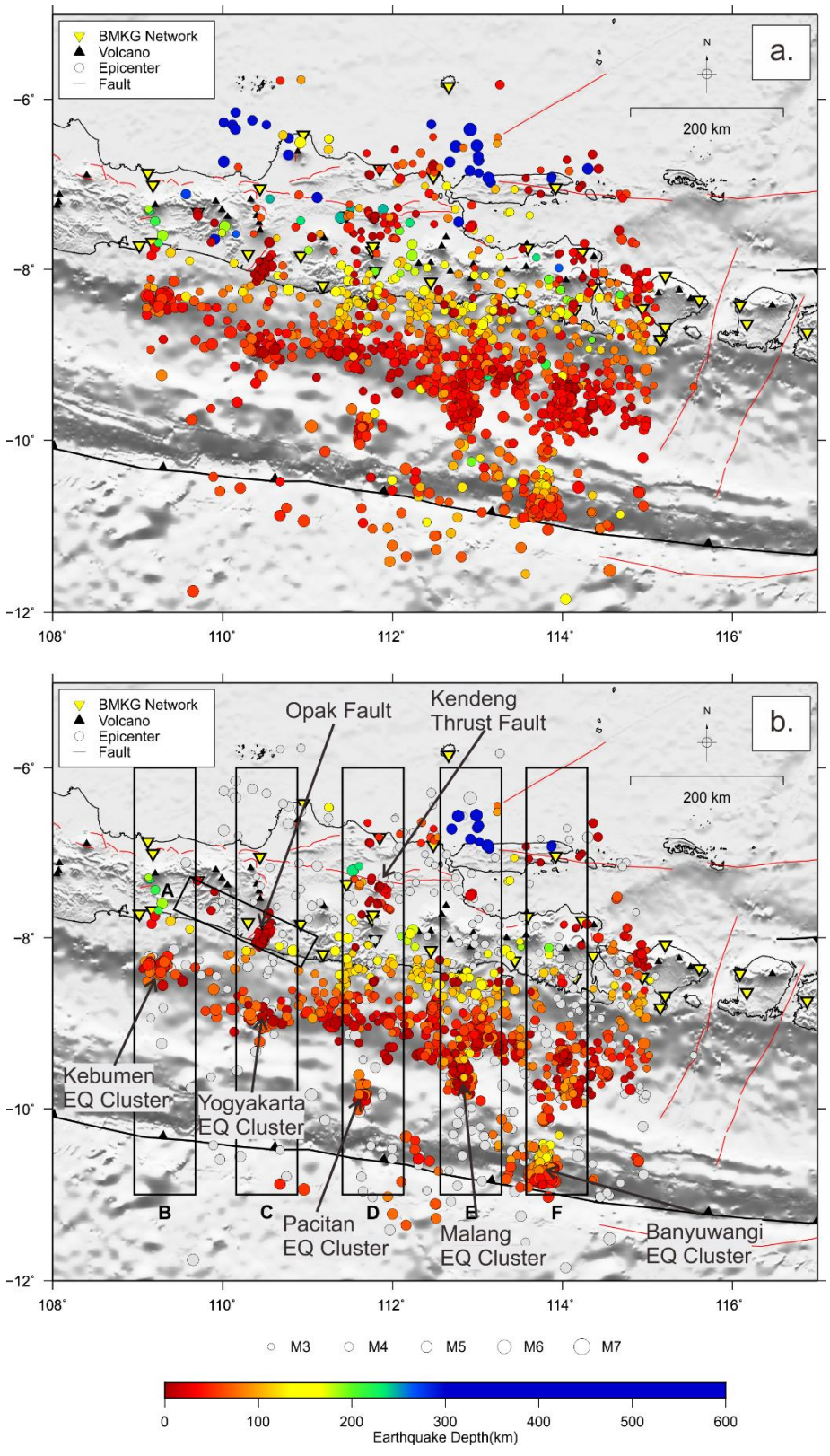
BMKG Network
Volcano
Epicenter
Fault
a.
N
200 km
−6°
−8°
−10°
−12°
108°
110°
112°
114°
116°
b.
Opak Fault
Kendeng
Thrust Fault
A
B
C
D
E
F
Kebumen
EQ Cluster
Yogyakarta
EQ Cluster
Pacitan
EQ Cluster
Malang
EQ Cluster
Banyuwangi
EQ Cluster
M3
M4
M5
M6
M7
0
100
200
300
400
500
600
Earthquake Depth(km)

535 Fig. 7. Comparison of seismic distribution in the Central and East Java region. **a** before
536 relocation. **b** after the relocation. Blocks A-F are the area used to plot the vertical cross-sections
537 shown in Fig 9. The solid-colored circles represent earthquake focus depth, while the grey
538 circles are earthquakes which were eliminated in the relocation process.

539

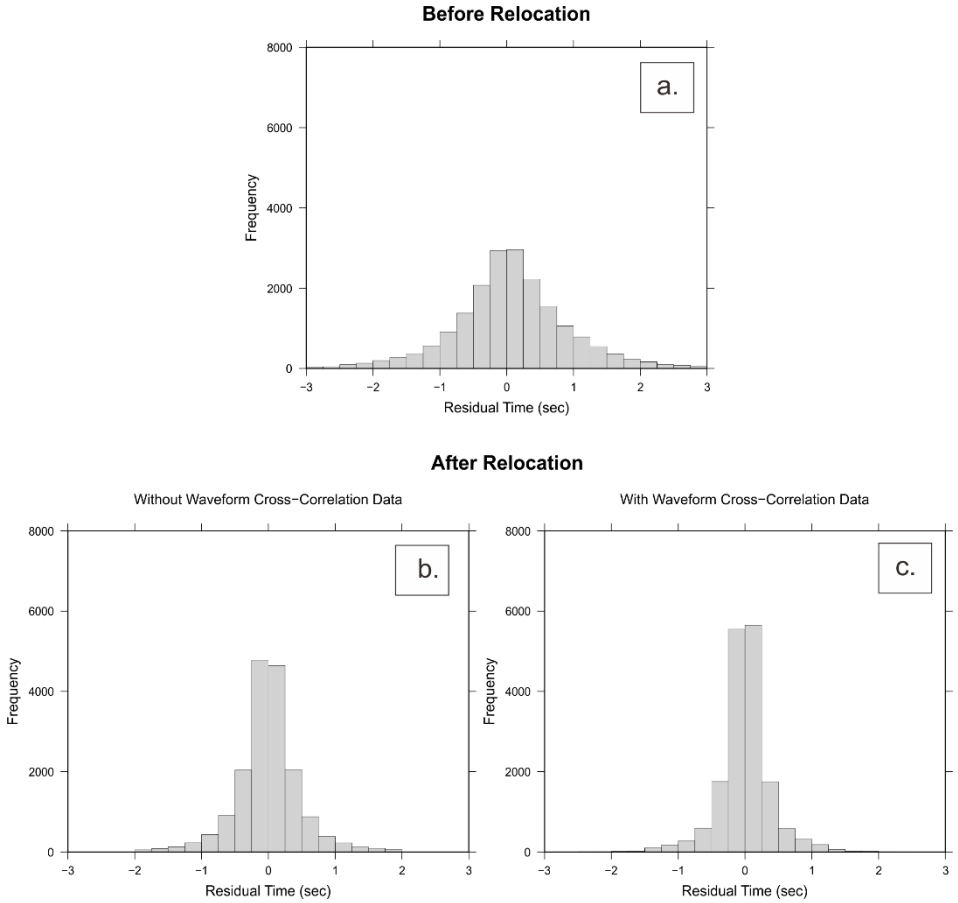

540

541 Fig. 8. **a** Histograms of travel time residuals before relocation and **b** after relocation; without

542 and **c** with waveform cross-correlation data in the relocation process of 1,127 events.

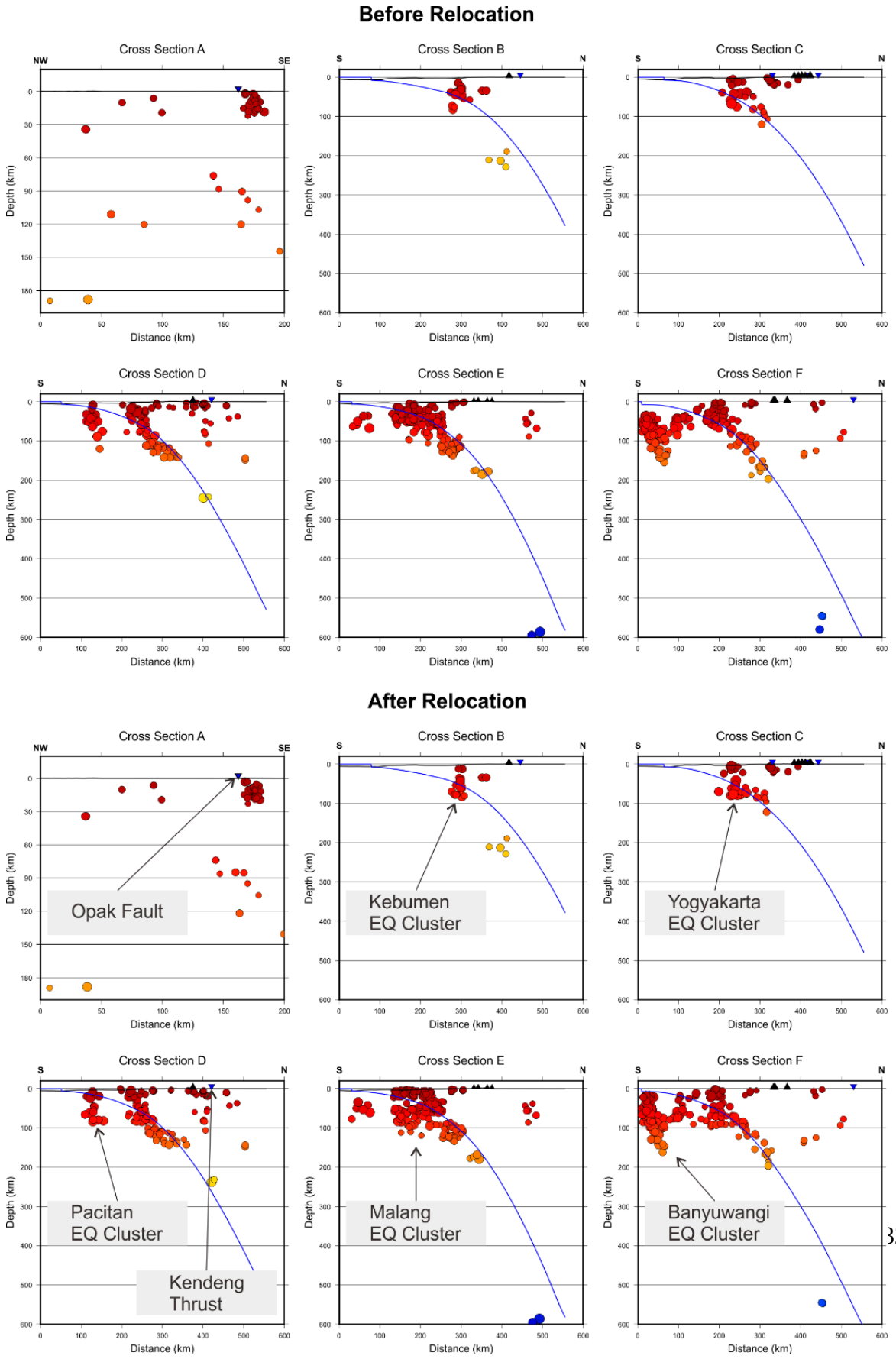

544 Fig. 9. Vertical cross-sections of blocks A-F before and after relocation (as shown in Figure 6).
545 These are along the Opak Fault, the Kebumen, Yogyakarta, Pacitan, Kendeng Thrust Fault,
546 and the Malang and Banyuwangi clusters. The blue line indicates the slab 1.0 model (Hayes et
547 al. 2012).

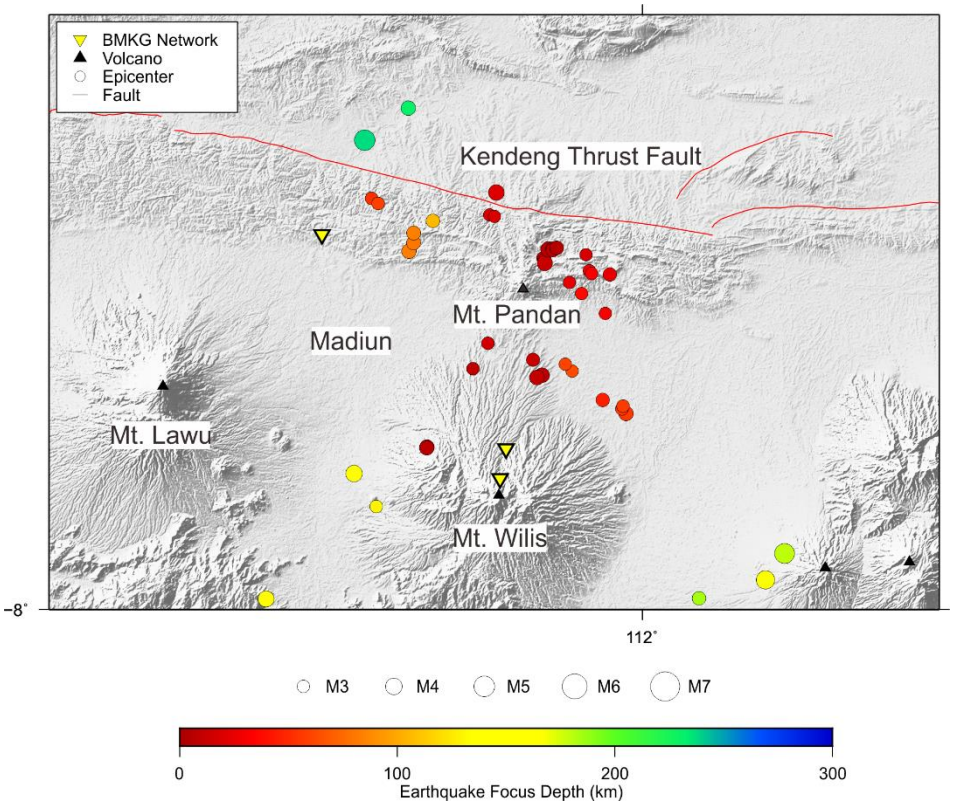

Fig. 10. Map of seismic distribution around Mt. Pandan and the Kendeng Thrust Fault north of Madiun, East Java, Indonesia.

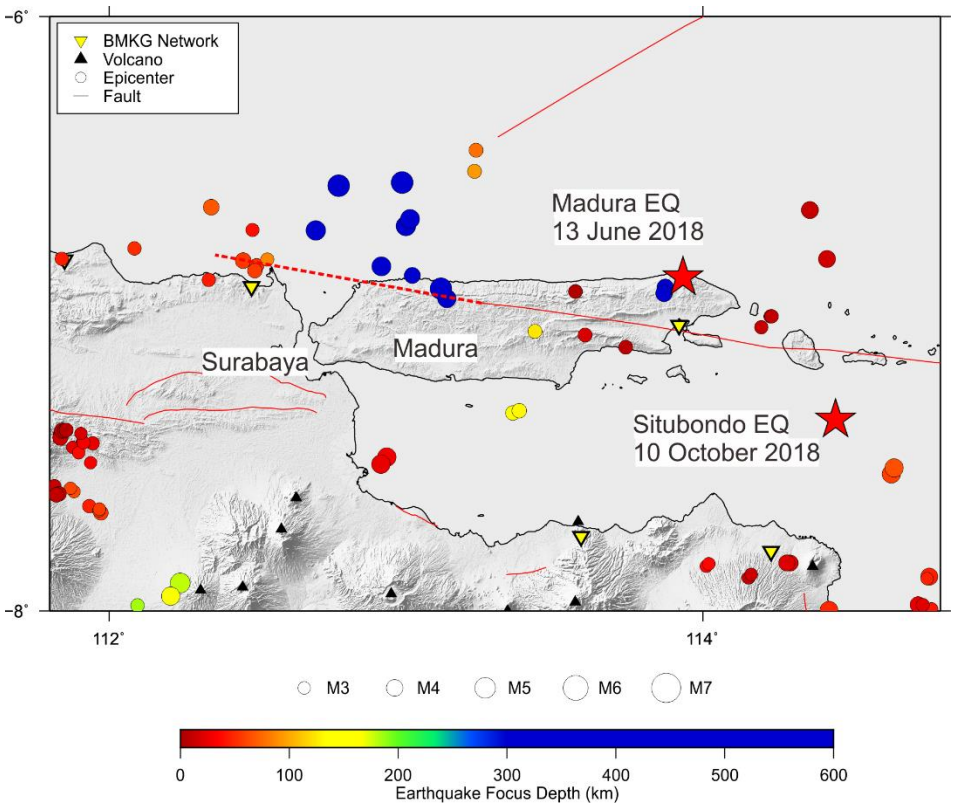

Fig. 11. Map of seismic distribution in the Rembang and Madura areas. The dashed red line is a possible extended fault. Red stars are recently earthquakes that occurred in 2018.

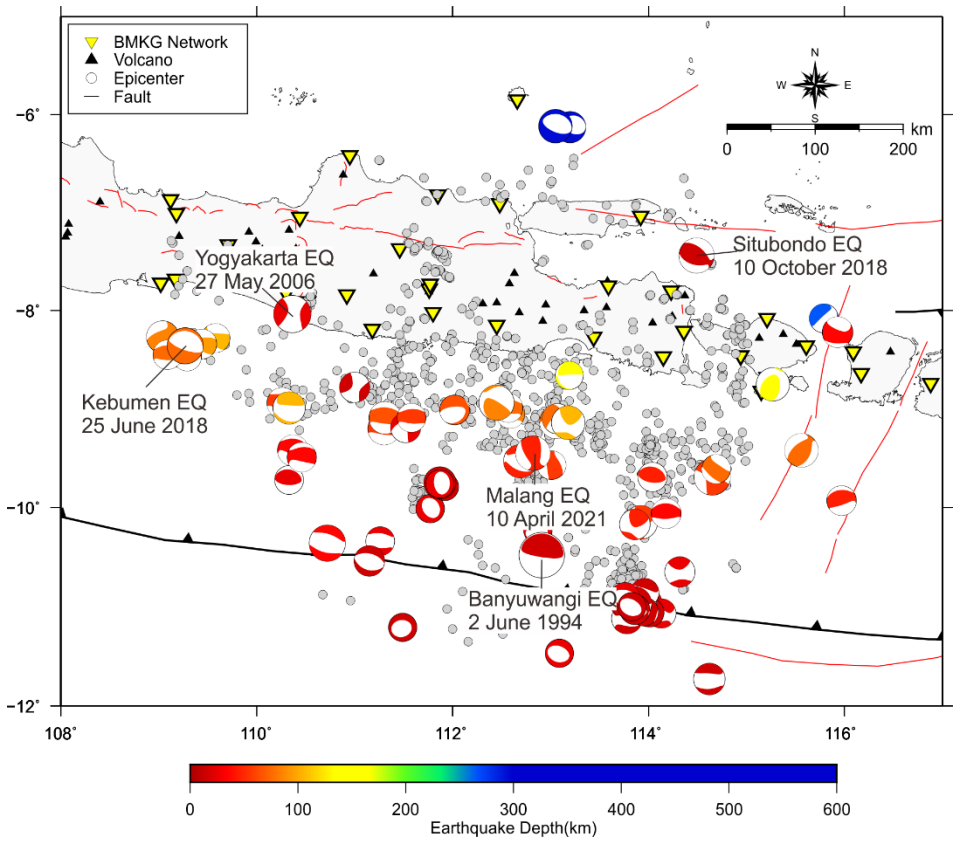

Fig. 12. Map of focal mechanism distribution in Central and East Java, taken from the Global Centroid Moment Tensor (GCMT) (Dziewonski et al. 1981; Ekström et al. 2012) (https://www.globalcmt.org/) during the time period 2009 to 2018. Grey dots are relocated epicentres.